

Direct structural evidences of Mn₁₁Ge₈ and Mn₅Ge₂ clusters in Ge_{0.96}Mn_{0.04} thin films

Yong Wang, Jin Zou, Zuoming Zhao, Xinhai Han, Xiaoyu Zhou, and Kang L. Wang

Citation: *Applied Physics Letters* **92**, 101913 (2008); doi: 10.1063/1.2884527

View online: <http://dx.doi.org/10.1063/1.2884527>

View Table of Contents: <http://scitation.aip.org/content/aip/journal/apl/92/10?ver=pdfcov>

Published by the [AIP Publishing](#)

Articles you may be interested in

[Novel structures and physics of nanomagnets \(invited\)](#)

J. Appl. Phys. **117**, 172609 (2015); 10.1063/1.4914339

[The early stage of formation of self-organized nanocolumns in thin films: Monte Carlo simulations versus atomic-scale observations in Ge-Mn](#)

J. Appl. Phys. **115**, 053515 (2014); 10.1063/1.4864271

[Direct evidence for abrupt postcrystallization germanium precipitation in thin phase-change films of Sb – 15 at. % Ge](#)

Appl. Phys. Lett. **93**, 071906 (2008); 10.1063/1.2970106

[Effect of growth temperature on morphology, structure and luminescence of Eu-doped GaN thin films](#)

Appl. Phys. Lett. **85**, 4890 (2004); 10.1063/1.1825619

[Magnetic and structural properties of GaN thin layers implanted with Mn, Cr, or V ions](#)

J. Appl. Phys. **96**, 5663 (2004); 10.1063/1.1805718

The advertisement for Goodfellow features a collage of various materials and components. On the left, there are red and white pills. In the center, there are small metal parts and a blue component. On the right, there are various powders, granules, and a yellow component. The text is overlaid on the left side of the collage.

Pure Metals • Ceramics
Alloys • Polymers
in dozens of forms

Goodfellow

Small quantities *fast* • Expert technical assistance • 5% discount on online orders

Direct structural evidences of $Mn_{11}Ge_8$ and Mn_5Ge_2 clusters in $Ge_{0.96}Mn_{0.04}$ thin films

Yong Wang,¹ Jin Zou,^{1,a)} Zuoming Zhao,² Xinhai Han,² Xiaoyu Zhou,² and Kang L. Wang²

¹School of Engineering and Centre for Microscopy and Microanalysis, The University of Queensland, Brisbane QLD 4072, Australia

²Electrical Engineering Department, University of California at Los Angeles, Los Angeles, California 90095, USA

(Received 11 December 2007; accepted 30 January 2008; published online 11 March 2008)

Mn-rich clusters in Mn-doped Ge thin films epitaxially grown on Ge (001) have been investigated by various transmission electron microscopy techniques. Both the mysterious $Mn_{11}Ge_8$ and the hexagonal Mn_5Ge_2 ($a=0.72$ nm and $c=1.3$ nm) clusters were confirmed to coexist in the thicker $Ge_{0.96}Mn_{0.04}$ film (80 nm). Their possible formation mechanism is attributed to the existence of ordered stacking faults. The fact that no Mn-rich clusters found in thinner films (≤ 40 nm) suggests that, for a given Mn concentration and growth/annealing condition, a critical thickness exists for the formation of Mn-rich clusters. © 2008 American Institute of Physics.

[DOI: 10.1063/1.2884527]

Diluted magnetic semiconductor (DMS) has been investigated extensively due to its promising applications in spintronic devices.^{1,2} In particular, Ge_xMn_{1-x} DMS has attracted considerable attention.²⁻⁹ Many attempts have been devoted to obtaining a room-temperature ferromagnetic Ge_xMn_{1-x} DMS with high concentration and uniformly distributed Mn.³⁻⁹ However, the fact of the low solubility of Mn in Ge makes it a challenge task to secure a high Curie temperature DMS. Therefore, the knowledge of Mn distribution is essential to understand the origin of ferromagnetism of Ge_xMn_{1-x} DMS films. It has been reported that inhomogeneous Mn distributed in Ge films tends to form Mn-rich magnetic precipitates,⁶⁻⁸ such as Mn_3Ge_3 and $Mn_{11}Ge_8$.¹⁰ Jamet *et al.*¹¹ and Li *et al.*⁹ found nanosized Mn-rich GeMn columns in the GeMn films grown on Ge. Bihler *et al.*⁶ and Passacantando *et al.*⁸ reported Mn_5Ge_2 clusters in the epitaxially grown GeMn films and the ion implanted GeMn alloys. In contrast, Park *et al.*¹² and Biegger *et al.*¹³ deduced the existence of $Mn_{11}Ge_8$ ferromagnetic clusters in the GeMn thin films, based on the ratio of Mn and Ge concentration and the extraordinary magnetic properties found in their GeMn films.

In this letter, the $Ge_{0.96}Mn_{0.04}$ thin films grown on Ge (001) with different thickness were investigated using transmission electron microscopy (TEM), energy dispersive spectroscopy (EDS), and energy filtered TEM (EFTEM). From which, we confirmed the existence of the orthorhombic $Mn_{11}Ge_8$ clusters in the thicker $Ge_{0.96}Mn_{0.04}$ thin films. Furthermore, hexagonal Mn_5Ge_2 clusters were also discovered that coexist with the $Mn_{11}Ge_8$ clusters in the thicker $Ge_{0.96}Mn_{0.04}$ thin film. The effect of the film thickness on the formation of these Mn-rich clusters is discussed.

The $Ge_{0.96}Mn_{0.04}$ thin films with nominal thickness of 80, 40, and 20 nm were grown on Ge (001) substrates by a Perkin-Elmer solid source molecular beam epitaxy system. Ge substrates were firstly degreased by acetone and methanol with ultrasonic agitation. The substrates were then etched in 1% HF for 1 min and loaded into the vacuum chamber after drying by N_2 . The native oxide was removed by a 550 °C

annealing for 10 min in the chamber. The surface quality of the substrate was monitored to have 2×1 reconstruction by the *in situ* reflection high energy electron diffraction patterns.¹⁴ Prior to the thin film deposition, a 10 nm Ge buffer layer was grown at 400 °C. After that, 4% Mn-doped Ge was deposited on the Ge substrates with a growth rate of 0.02 nm/s at 70 or 120 °C, although no structural difference can be detectable for samples grown at different temperatures. After the growth, the samples were further annealed at 400 °C for 30 min in the chamber.

TEM investigations were carried out to understand the nanostructures and compositional variations of grown thin films. $\langle 110 \rangle$ cross-sectional TEM specimens were prepared using a tripod technique, followed by final ion polishing. The TEM and EFTEM were performed in a FEI Tecnai F30 TEM equipped with a Gatan image filtering system. The EDS was carried out in a FEI Tecnai F20 TEM in scanning TEM (STEM) mode.

Figure 1(a) is a typical cross-sectional TEM image and shows a general morphology of the $Ge_{0.96}Mn_{0.04}$ thin film

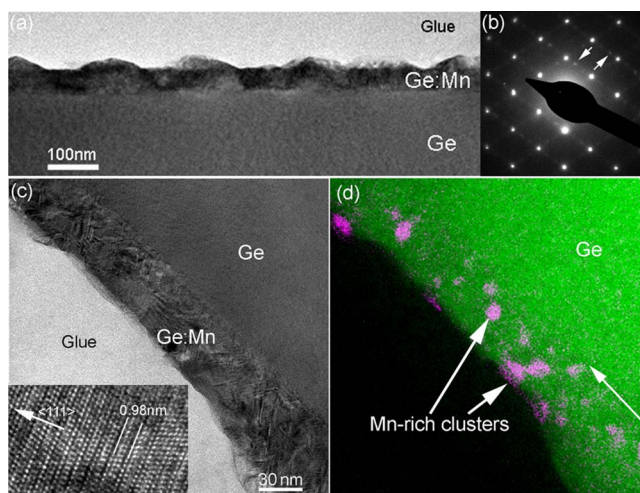


FIG. 1. (Color online) (a) A typical TEM image of the sample with nominal thickness of 80 nm. (b) The SAED pattern with a feature of ordered stacking faults (arrowed). (c) A high magnification TEM image with the inset displaying the stacking faults. (d) The corresponding EFTEM elemental mapping of (c) showing Mn-rich clusters.

^{a)} Author to whom correspondence should be addressed. Electronic mail: j.zou@uq.edu.au.

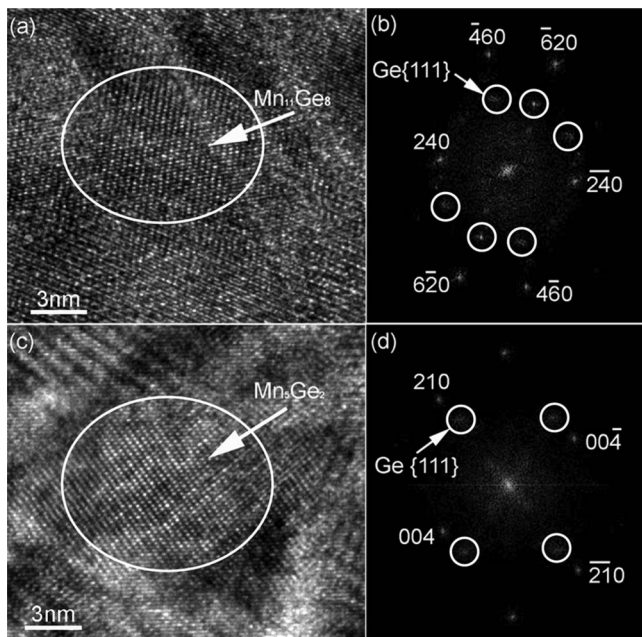


FIG. 2. (a) A HRTEM image showing a $\text{Ge}_3\text{Mn}_{11}$ cluster in the thicker sample (80 nm). (b) The FFT pattern of (a). (c) A typical HRTEM image of a Ge_2Mn_5 cluster in the thicker sample. (d) The FFT pattern of (c).

with the nominal thickness of 80 nm. In Fig. 1(a), a thin film with a rough surface is observed. This rough surface is believed to be caused by the relatively higher growth rate.¹⁴ Figure 1(b) is a selected area electron diffraction (SAED) pattern taken along the $[1\bar{1}0]_{\text{Ge}}$ direction, showing a characteristic of the diamond structure with ordered stacking faults (SFs) [arrowed in Fig. 1(b)], similar to those observed in I-doped (Zn,Cr)Te films.¹⁵ To obtain the detailed structural information, high magnification TEM was carried out and a typical $[1\bar{1}0]$ zone-axis TEM image is shown on Fig. 1(c), in which a high density of SFs can be seen in the entire film. High resolution TEM (HRTEM) was used to confirm the ordered SFs. Such an example is presented in the inset of Fig. 1(c), in which a triplet periodicity of 0.98 nm (which is $3 \times$ the $\{111\}_{\text{Ge}}$ lattice spacing) of the ordered SFs is explicitly featured. To determine the distribution of Mn in the $\text{Ge}_{0.96}\text{Mn}_{0.04}$ thin film, EFTEM was performed.¹⁶ Figure 1(d) is an overlapped elemental map that corresponds to Fig. 1(c) with Mn in the light contrast. From the elemental map, Mn-rich clusters with the size of several nanometers can be observed to be randomly distributed in the entire $\text{Ge}_{0.96}\text{Mn}_{0.04}$ film. To determine Mn concentration within different thin films, EDS was carried out in STEM mode (with a probe size in the range of 2 nm). EDS results from over a dozen points taken from the thinner film (no Mn clusters were found) showed the average Mn concentration of $\sim 4\%$, which is identical to the nominal value. However, for the thicker film (80 nm), the highest Mn concentration reaches $\sim 14\%$ (in the area with clusters) and the lowest is only $\sim 0.5\%$ in the film, indicating the far inhomogeneous Mn distribution in the thicker film.

In order to determine the crystalline phase(s) of observed Mn-rich clusters, HRTEM was again carried out. Extensive HRTEM investigation confirmed the existence of two types of GeMn clusters. Figure 2(a) shows an example, in which a cluster can be seen. It should be noted that the matrix was sliced off from its $\langle 110 \rangle$ zone axis in order to obtain a better

HRTEM image for the cluster. To determine the crystal structure of the cluster, the fast Fourier transformation (FFT) (equivalent to the electron diffraction) of Fig. 2(a) was performed^{6,17} and is shown in Fig. 2(b). From the FFT pattern, a set of diffraction pattern overlapped with several diffraction spots can be seen. Through reversed FFT (not shown here), we confirmed that the set of diffraction pattern came from the cluster and the additional diffraction spots resulted from $\{111\}$ atomic planes [circled in Fig. 2(b)] of the GeMn matrix. Using the lattice spacing of the matrix as the reference, we then can calculate the observed lattice spacings of the cluster, which match well with $\{240\}$, $\{6\bar{2}0\}$, and $\{4\bar{6}0\}$ atomic planes of the orthorhombic $\text{Mn}_{11}\text{Ge}_8$ phase with the lattice parameters of $a=1.320$ nm, $b=1.588$ nm, and $c=0.509$ nm.¹⁸ To further confirm the cluster belonging to the $\text{Mn}_{11}\text{Ge}_8$ phase, the crystallographic angles between these atomic planes were measured and the results also fit perfectly with the corresponding theoretical crystallographic angles of the $\text{Mn}_{11}\text{Ge}_8$ phase.

In this study, another type GeMn cluster has also been identified in the thicker GeMn film. Figures 2(c) and 2(d) show such an example, in which Fig. 2(c) is a typical HRTEM image and Fig. 2(d) is the corresponding FFT pattern. Both the HRTEM and FFT suggest that the cluster belongs to the hexagonal Mn_5Ge_2 phase with the lattice parameters of $a=0.720$ nm and $c=1.307$ nm.¹⁹ In Fig. 2(d), two sets of diffraction patterns can be distinguished with one belonging to the $\langle 1\bar{1}0 \rangle$ zone axis of the matrix (the $\{111\}$ planes are circled) and the other set can be uniquely indexed as the diffraction pattern of $\langle 1\bar{2}0 \rangle$ zone axis of the hexagonal Mn_5Ge_2 phase. The fact that the diffraction spots of 220^*_{Matrix} is coincided with the diffraction spots of $214^*_{\text{Mn}_5\text{Ge}_2}$ indicates that there is a crystallographic orientation relationship between the hexagonal Mn_5Ge_2 phase and the $\text{Ge}_{0.96}\text{Mn}_{0.04}$ matrix. Through detailed analysis of the FFT pattern shown in Fig. 2(d), combining with the HRTEM image, the crystallographic orientation relationship between the Mn_5Ge_2 clusters and the $\text{Ge}_{0.96}\text{Mn}_{0.04}$ matrix can be determined as $\langle 210 \rangle_{\text{Ge}_2\text{Mn}_5} \parallel \langle 111 \rangle_{\text{Matrix}}$ and $\langle 1\bar{2}0 \rangle_{\text{Ge}_2\text{Mn}_5} \parallel \langle 1\bar{1}0 \rangle_{\text{Matrix}}$. Our extensive HRTEM investigations suggest no other type Mn-rich clusters in the GeMn films.

HRTEM investigations have been repeated on the samples with the nominal thickness of 20 and 40 nm, as shown in Figs. 3(a) and 3(b), respectively. No noticeable Mn-rich clusters are observed in these thinner GeMn films. Interestingly, strain (dark) contrasts can be seen in the film with the nominal thickness of 40 nm [as marked in Fig. 3(b)], suggesting a possible elemental segregation.²⁰ It is also of interest to note that Mn-rich nanosized columns were observed in the 40 nm thin film without annealing [Fig. 3(c)], which is similar to previously reported.^{11,9} This result indicates that postannealing at 400 °C makes the nanosized columns evolve into the clusterlike dark regions. Since Mn-rich clusters were only found in the 80 nm thick sample, we anticipate that these dark regions might have a slightly higher Mn concentration. Nevertheless, the entire film remains the diamond structure and extensive TEM observations found no Mn-rich clusters in these samples, indicating that the nominal thickness of the thin film plays a critical role in the formation of the Mn-rich clusters. Since the nominal composition of all three thin films is the same, i.e., $\text{Ge}_{0.96}\text{Mn}_{0.04}$, the

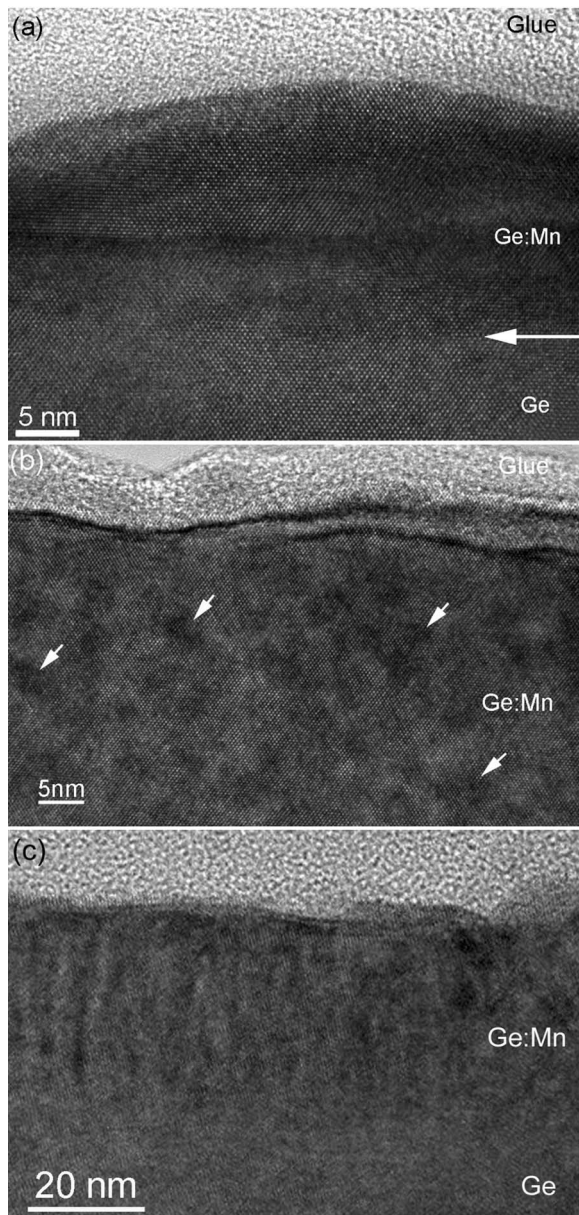


FIG. 3. Typical HRTEM images of the $\text{Ge}_{0.96}\text{Mn}_{0.04}$ films with nominal thicknesses of 20 nm (annealed) (a), 40 nm (annealed) (b), and 40 nm (nonannealed) (c).

thicker thin film must provide more Mn atoms in the entire thin film. The fact that the GeMn clusters were only found in the thicker (80 nm) film suggests that the formation of Mn-rich clusters can only take place when sufficient Mn is available for nucleation.⁶

It should be noted that the commonly reported Mn_5Ge_3 clusters were not observed in our case, although we cannot absolutely rule out the existence of the Mn_5Ge_3 clusters based on the limitation of TEM. To better understand this phenomenon, we note that, unlike previous reports,^{6–10} a high density of ordered SFs (refer to Fig. 1) were observed within the entire thin film in our case. These SFs are closely related to the growth parameters such as growth rate, growth temperature, and annealing process. For example, SFs will more easily be formed when the growth rate is high and, in turn, might affect the Mn diffusion and the subsequent formation of the Mn-rich clusters. If this is true, this study indicates that the nature of defects may also have an impact on the

formation and the kind of Mn-rich clusters in the GeMn thin film. On the other hand, it has been found that the Mn_5Ge_3 phase could transform into the $\text{Mn}_{11}\text{Ge}_8$ phase during annealing,²¹ meaning that postannealing might also play an important role in the formation and the kind of Mn-rich clusters.

In summary, Mn-rich clusters in the 80 nm thick $\text{Ge}_{0.96}\text{Mn}_{0.04}$ film grown on Ge (001) substrates have been identified. The mysterious $\text{Mn}_{11}\text{Ge}_8$ clusters were found in the film. Besides, hexagonal Mn_5Ge_2 clusters have been also determined in this thin film. The Mn_5Ge_2 clusters have a certain crystallographic orientation relationship with the $\text{Ge}_{0.96}\text{Mn}_{0.04}$ matrix. The fact that no Mn-rich clusters were found in thinner GeMn films suggests that, for a given nominal Mn concentration, there exists a critical thickness h (in our case, $40 \text{ nm} < h < 80 \text{ nm}$). Below that, Mn-rich clusters cannot be nucleated, possibly due to insufficient total Mn content in the GeMn film.

The Australia Research Council, Focus Center Research Program—Center on Functional Engineered Nano Architectonics, and Western Institution of Nanoelectronics are acknowledged for their financial support of this project.

¹H. Ohno, *Science* **281**, 951 (1998).

²Y. D. Park, A. T. Hanbicki, S. C. Erwin, C. S. Hellberg, J. M. Sullivan, J. E. Mattson, T. F. Ambrose, A. Wilson, G. Spanos, and B. T. Jonker, *Science* **295**, 651 (2002).

³J. S. Kang, G. Kim, S. C. Wi, S. S. Lee, S. Choi, S. Cho, S. W. Han, K. H. Kim, H. J. Song, H. J. Shin, A. Sekiyama, S. Kasai, S. Suga, and B. I. Min, *Phys. Rev. Lett.* **94**, 147202 (2005).

⁴Y. X. Chen, S. S. Yan, Y. Fang, Y. F. Tian, S. Q. Xiao, G. L. Liu, Y. H. Liu, and L. M. Mei, *Appl. Phys. Lett.* **90**, 052508 (2007).

⁵P. De Padova, J. P. Ayoub, I. Berbezier, J. M. Mariot, A. Taleb-Ibrahimid, M. C. Richtere, O. Heckmanne, A. M. Testaf, D. Fioranif, B. Olivierig, S. Picozzih, and K. Hricovinie, *Surf. Sci.* **601**, 2628 (2007).

⁶C. Bihler, C. Jaeger, T. Vallaitis, M. Gjukic, M. S. Brandt, E. Pippel, J. Woltersdorf, and U. Gosele, *Appl. Phys. Lett.* **88**, 112506 (2006).

⁷S. Ahlers, D. Bougeard, N. Sircar, G. Abstreiter, A. Trampert, M. Opel, and R. Gross, *Phys. Rev. B* **74**, 214411 (2006).

⁸M. Passacantando, L. Ottaviano, F. D'Orazio, F. Lucari, M. De Biase, G. Impellizzeri, and F. Priolo, *Phys. Rev. B* **73**, 195207 (2006).

⁹A. P. Li, C. Zeng, K. Van Benthem, M. F. Chisholm, J. Shen, S. V. S. Nageswara Rao, S. K. Dixit, L. C. Feldman, A. G. Petukhov, M. Foygel, and H. H. Weitering, *Phys. Rev. B* **75**, 201201 (2007).

¹⁰H. Li, Y. Wu, Z. Guo, P. Luo, and S. Wang, *J. Appl. Phys.* **100**, 103908 (2006).

¹¹M. Jamet, D. Barski, T. Devillers, V. Poydenot, R. Dujardin, P. Bayle-Geillemaud, J. Rothman, E. Bellet-Amalric, A. Marty, J. Cibert, R. Matana, and S. Tatarenko, *Nat. Mater.* **5**, 653 (2006).

¹²Y. D. Park, A. Wilson, A. T. Hanbicki, J. E. Mattson, T. Ambrose, G. Spanos, and B. T. Jonker, *Appl. Phys. Lett.* **78**, 2739 (2001).

¹³E. Biegger, L. Staheli, M. Fonin, U. Rudiger, and Yu. S. Dedkov, *J. Appl. Phys.* **101**, 103912 (2007).

¹⁴A. P. Li, J. F. Wendelken, J. Shen, L. C. Feldman, J. R. Thompson, and H. H. Weitering, *Phys. Rev. B* **72**, 195205 (2005).

¹⁵S. Kuroda, N. Nishizawa, K. Takita, M. Mitome, Y. Bando, K. Osuch, and T. Dietl, *Nat. Mater.* **6**, 440 (2007).

¹⁶X. Z. Liao, J. Zou, D. Cockayne, J. Wan, Z. M. Jiang, G. Jin, and K. L. Wang, *Appl. Phys. Lett.* **79**, 1258 (2001).

¹⁷Y. Wang, X. L. Du, Z. X. Mei, Z. Q. Zeng, M. J. Ying, H. T. Yuan, J. F. Jia, Q. K. Xue, and Z. Zhang, *Appl. Phys. Lett.* **87**, 051901 (2005).

¹⁸N. Yamada, K. Maeda, Y. Usami, and T. Ohoyama, *J. Phys. Soc. Jpn.* **55**, 3721 (1986).

¹⁹T. Matsui, M. Shigematsu, S. Mino, H. Tsuba, H. Mabuchi, and K. Morii, *J. Magn. Magn. Mater.* **192**, 247 (1999).

²⁰D. Bougeard, S. Ahlers, A. Trampert, N. Sircar, and G. Abstreiter, *Phys. Rev. Lett.* **97**, 237202 (2006).

²¹Y. M. Cho, S. S. Yu, Y. E. Ihm, D. Kim, H. Kim, J. S. Baek, C. S. Kim, and B. T. Lee, *J. Magn. Magn. Mater.* **282**, 385 (2004).